



International Conference on Concentrating Solar Power and Chemical Energy Systems,
SolarPACES 2014

Numerical investigation of PCM-based thermal energy storage system

Selvan Bellan^a, Jose Gonzalez-Aguilar^{a*}, Manuel Romero^a, Muhammad M. Rahman^{b,c},
D. Yogi Goswami^{b,d}, Elias K. Stefanakos^{b,e}

^aIMDEA Energy Institute, Ramon de la Sagra 3, Móstoles 28935, Spain

^bClean Energy Research Center, University of South Florida, 4202 E. Fowler Ave., Tampa, FL 33620, USA

^cDepartment of Mechanical Engineering, University of South Florida, 4202 E. Fowler Ave., Tampa, FL 33620, USA

^dDepartment of Chemical & Biomedical Engineering, USF, 4202 E. Fowler Ave., Tampa, FL 33620, USA

^eDepartment of Electrical Engineering, University of South Florida, 4202 E. Fowler Ave., Tampa, FL 33620, USA

Abstract

A latent thermal energy storage system, which consists of sodium nitrate filled spherical capsules in a cylindrical tank, is analyzed for concentrating solar power plant applications. The high temperature synthetic oil, Therminol 66, is used as heat transfer fluid. A numerical model is developed to investigate the behavior of the system. The developed model is validated using the reported experimental and numerical data. The influence of capsule size and the flow rate of heat transfer fluid (HTF) on the temperature distribution, fluid flow, melting and solidification of the system is studied. The natural convection effect present in the liquid region during melting is resolved by the effective thermal conductivity, which is calculated by enthalpy formulation method. The results indicated that the heat transfer rate is increased and eventually the charging/discharging time is decreased when the capsule size is decreased, or the HTF flow rate is increased.

© 2015 The Authors. Published by Elsevier Ltd. This is an open access article under the CC BY-NC-ND license (<http://creativecommons.org/licenses/by-nc-nd/4.0/>).

Peer review by the scientific conference committee of SolarPACES 2014 under responsibility of PSE AG

Keywords: Latent thermal energy storage, Thermocline system, Encapsulated phase change material, Molten salt, Concentrating solar power

* Corresponding author. Tel.: +34-917371120.

E-mail address: jose.gonzalez@imdea.org; selvan.bellan@imdea.org

Nomenclature

C_p	specific heat (J/kg·K)
d	diameter of the capsule (m)
h_f	heat transfer coefficient (W/m ² ·K)
L	latent heat of fusion (J/kg)
Nu	Nusselt number
P	pressure (Pa)
Pr	Prandtl number
r	radial coordinate (m)
r_c	outer radius of inner layer coating (m)
r_i	inner radius of the capsule (m)
r_m	solid-liquid interface (m)
r_o	outer radius of the capsule (m)
R	storage tank radius (m)
Ra	Rayleigh number
t	time (s)
T	temperature (K)
\mathbf{u}	velocity vector (m/s)
z	axial coordinate (m)

Greek symbols

γ	melt fraction at each element
η	dynamic viscosity (Pa·s)
λ	thermal conductivity (W/m·K)
ρ	density (kg/m ³)

Subscripts

eff	effective
f	fluid
i	inner
$init$	initial
liq	liquid phase
m	melting
nik	nickel
o	outer
pol	polymer
s	solid
sol	solid phase

Abbreviations

CHTZ	constant high temperature zone
CLTZ	constant low temperature zone
CMTZ	constant melt temperature zone
CSP	concentrated solar power
HEZ	heat exchange zone
HTF	heat transfer fluid
PCM	phase change material
R&D	research and development
TES	thermal energy storage

1. Introduction

Thermal energy storage plays an important role in concentrating solar power (CSP) plants. Thus, significant R&D activities are being developed in the field of thermal energy storage (TES) in recent years. Numerous storage methods for various temperature ranges have been investigated and reviewed [1-2]. At present, latent heat storage in phase change materials (PCM) is considered as one of the most attractive methods. Several PCMs have been identified for low [3] and high temperatures [4] applications and experimental and numerical studies have been conducted to characterize them. Garg et al. [5] summarized early literatures on packed bed thermal storage systems. The results of various numerical models of both sensible and latent heat storage methods were compared by Ismail and Stuginsky [6]. Reviews on PCM based thermocline storage systems were presented [7-8]. Various numerical models have been developed in the past few decades to predict the thermal and hydrodynamic behavior and performance of the packed bed latent heat thermal energy storage systems. These models are generally classified into three major groups: Single phase model, two phase continuous solid phase model and the concentric dispersion model. Since the detail modeling of each element inside the system is so complicated due to its complex configuration and process dynamics, many hypotheses and correlations have been used in these models. To improve the accuracy of the model, an effective model has been developed and reported recently [9], which is different from the previous models. In this model, the fluid flow through the voids among the PCM spheres and the thermal gradients inside the capsules can be investigated. Experimental correlations or empirical expressions are not involved in this model except the treatment of the effective thermal conductivity, which is used to include the natural convection effects in the liquid PCM during melting. Although several studies have been reported in the literature on thermal energy storage systems, phase change process, heat transfer characteristics inside the packed bed and thermal gradients inside the capsules at high temperatures have not been studied completely. Accordingly, in this study, the effective packed bed model is used to investigate the thermal behavior and performance of the TES system. Temperature distribution, fluid flow, melting and solidification of the system are predicted and the influence of system configuration and operating parameters on the performance of the system is studied.

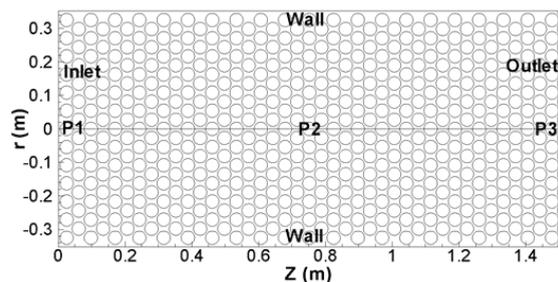


Fig.1. Schematic of the computational domain

2. Numerical modelling

2.1. Modelling approach and governing equations

Fig. 1 shows the schematic of a lab-scale thermal storage tank packed by spherical capsules. The capsules are filled with sodium nitrate, and the shell of the capsule is made up of nickel. Since the tendency of the sodium nitrate-shell interface is highly corrosive, a polymer coating is made at the inner surface of the shell to avoid contact between the sodium nitrate and shell. The high temperature synthetic oil, Therminol 66, is used as heat transfer fluid. In order to simulate the fluid flow and heat transfer inside the tank, a numerical model is developed based on the following assumptions: Due to the axial symmetry configuration and boundary conditions, the 2D model is adopted. The flow inside the tank is assumed as laminar and incompressible and the radiation heat transfer between the capsules is negligible. The rhombic packing is assumed, as a result, the contact between the capsules is point-to-point, and eventually the heat transfer between the capsules is negligible. Therefore, the void space between the capsules is assumed, because the 2D model does not lead to flow through the bed if the capsules contact to each

other [9]. Based on the foregoing assumptions, the governing equations to predict the heat transfer and fluid flow in the void region of the system are given by

$$\frac{\partial \rho_f}{\partial t} + \nabla \cdot (\rho_f \mathbf{u}) = 0 \quad (1)$$

$$\rho_f \frac{\partial \mathbf{u}}{\partial t} + \rho_f (\mathbf{u} \cdot \nabla) \mathbf{u} = -\nabla P + \nabla \left[\mu (\nabla \mathbf{u} + (\nabla \mathbf{u})^T) - \frac{2}{3} \mu \nabla \mathbf{u} \right] \quad (2)$$

$$(\rho C_p)_f \frac{\partial T_f}{\partial t} + (\rho C_p)_f \mathbf{u} \cdot \nabla T_f = \nabla \cdot (\lambda_f \nabla T_f) \quad (3)$$

where \mathbf{u} , ρ , μ , P , C_p , T and λ are velocity vector, density, dynamic viscosity, pressure, specific heat, temperature and thermal conductivity respectively. The energy equation in the PCM region is given by

$$\frac{\partial (\rho h)_s}{\partial t} = \nabla \cdot (\lambda_s \nabla T_s) \quad (4)$$

Where, the specific enthalpy (h) is defined as the sum of the sensible enthalpy h_{sen} and enthalpy change due to phase change γL , where L and γ are the latent heat of the material and the melt fraction respectively. The subscript f and s represent the HTF domain and PCM domain respectively.

Table 1. Boundary conditions

Boundary	T	Vi
Inlet	$T_i(t)$	Mass flow rate (kg/s)
Outlet	$\partial T / \partial z = 0$	$\partial V_i / \partial z = 0$
Wall	$h_w(T_a - T)$	0

The temperature dependent thermo-physical properties of the PCM, HTF and shell of the capsule are obtained from the Ref. [2]. The thermal resistance caused by the shell of the capsule is included in the model. The boundary conditions are given in Table 1. Grid dependent tests were carried out in the preliminary calculations for various grid sizes; 0.001, 0.002 and 0.005 m. The grid size of 0.002 m was found to be adequate. All the governing equations are solved using the commercial CFD code FLUENT.

2.2. Determination of effective thermal conductivity

From the literature on melting and solidification processes of the PCM, it is noticed that the thermal conduction is the major heat transfer mechanism during solidification process, whereas natural convection plays a vital role during melting process [10-11]. Most of the melting process models only considered the thermal conduction due to complexity in describing the natural convection during melting process. In this study, the convective effect present in the liquid region is resolved by the effective thermal conductivity. To predict this, one dimensional conduction model for phase change process inside a capsule is developed by enthalpy formulation method, based on the literature models [12-13]. The governing equation and boundary conditions are given below

$$(\rho C_p)_s \frac{\partial T_s}{\partial t} = \lambda \left[\frac{\partial^2 T_s}{\partial r^2} + \frac{2}{r} \frac{\partial T_s}{\partial r} \right] \quad (5)$$

During charge mode, the temperature of the capsule is initially assumed at lower than melting point of the PCM. When the $t > 0$, the spherical capsule is subjected to the convective heating at the outer surface due to the temperature of the fluid, which is higher than the melting temperature. Boundary conditions at the external surface and the center of the sphere are given as follows

$$-\lambda \frac{\partial T_s}{\partial t} = \frac{T_s - T_f}{\left(\frac{r_i}{r_o}\right)^2 \frac{1}{h_f} + \frac{r_i^2}{\lambda_{nik}} \left(\frac{r_o - r_c}{r_c r_o}\right) + \frac{r_c - r_i}{\lambda_{pol}} \left(\frac{r_i}{r_c}\right)} \quad \text{at } r = r_i \quad \text{and} \quad \frac{\partial T_s}{\partial r} = 0 \quad \text{at } r = 0 \quad (6)$$

Where r_i , r_o and r_c are inner radius, outer radius and outer radius of the polymer layer of the capsule respectively. The hot heat transfer fluid heats up the capsule. When the temperature of the PCM close to the inner surface of the capsule reaches the melting temperature, the PCM melts and the liquid layer gradually grows up towards the center point of the capsule. The convection effect present in the molten PCM depends on the Rayleigh number, which is calculated by the thickness of the liquid layer ($L_a = r_i - r_m$). The effective thermal conductivity is calculated using Raithby's correlation [14],

$$\frac{\lambda_{eff}}{\lambda_{liq}} = 0.74 \left[\frac{\text{Pr}}{\text{Pr} + 0.861} \right]^{1/4} \left\{ \frac{\left(\frac{d_o - d_m}{2}\right) Ra_L}{(d_o d_m)^4 (d_m^{-7/5} + d_o^{-7/5})^5} \right\}^{1/4} \quad (7)$$

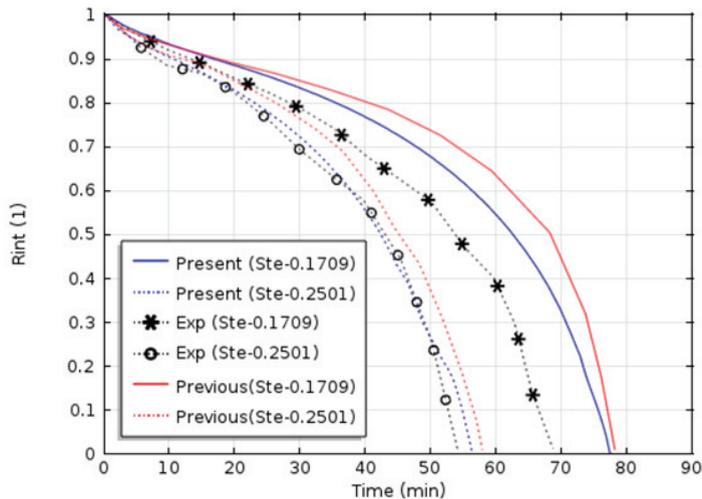


Fig. 2. Experimentally measured [13] and numerically predicted solid-liquid interface positions as a function of time for various Stefan numbers

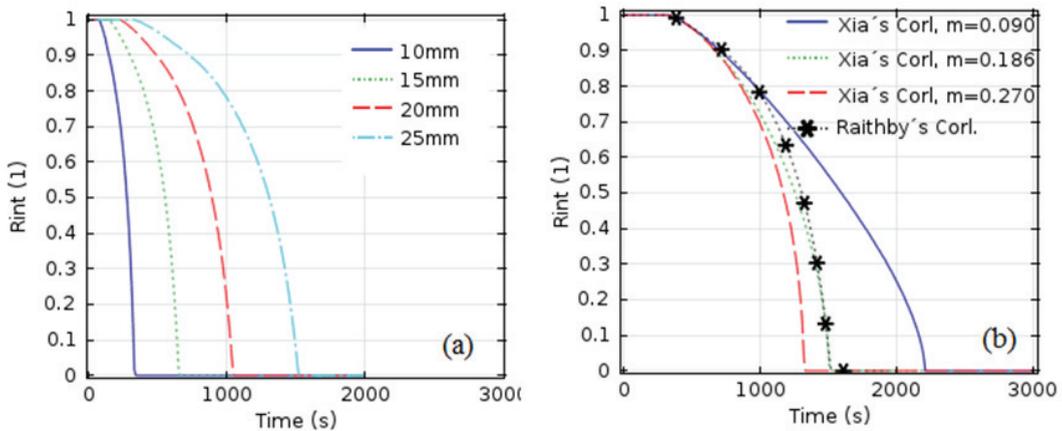


Fig. 3(a) Solid-liquid interface position as a function of time for different capsule sizes, (b) R_{int} position of 25 mm radius capsule predicted by Xia's correlation for various m coefficients.

The heat transfer coefficient (h_f) between the HTF and the spherical capsule is obtained from the empirical correlation [15]. In order to validate this model, present model results are compared with the reported experimental and numerical results [13]. In the reported investigation, the paraffin wax was filled in a spherical capsule, 49 mm radius, and placed inside a water filled vessel which was heated by an electrical heater; the melting process inside the capsule was studied and the temporal variation of solid-liquid interface position was predicted. In this study, simulations are performed for the same setup and conditions using the developed model. Fig. 2 shows the experimental and predicted values (present and previous models) of solid-liquid interface position as function of time for various Stefan numbers. The dimensionless interface position, R_{int} , is defined as the ratio of the interface radial distance (r_m) from the centre of the capsule to the inner radius of the capsule (r_i). As can be seen in the figure, the predicted and experimental interface positions are in close agreement in the initial stage whereas a significant deviation is found in the later stage. The main reason for this deviation could be the presence of 10% air gap in the capsule, but this model assumed as completely filled capsules. All in all, the present model results are comparable with previous model predictions and experimental measurements. Using the validated model, calculations are made for the present study; the solid-liquid interface position of the sodium nitrate filled capsule at P1 (as shown in Fig.1) is predicted. The convective heat flux boundary condition at the outer surface of the capsule is calculated according to the thermo-fluid flow at P1. Fig. 3 (a) shows the solid-liquid interface position as a function of time for different capsule sizes. As expected, the complete melting time is decreased when the capsule size is decreased. Here the effective thermal conductivity is calculated according to the solid-liquid interface position. This approach is appropriate for the melting problem of single capsule whereas which is complicated for the whole storage tank, because it is so complex to predict solid-liquid interface position for each capsule inside the tank. Thus, the Xia's correlation is adopted to calculate the effective thermal conductivity as given below [9, 16-17].

$$\frac{\lambda_{eff}}{\lambda_{liq}} = C Ra_L^m \quad (8)$$

In order to obtain the C and m coefficients, various values are assumed and their solid-liquid interface positions are predicted as a function of time. Then, the appropriate coefficients are obtained by comparing the R_{int} position and complete melting time obtained by Raithby's correlation (Eq. 7). Initially, the coefficient of C is fixed at 0.18 [9], and calculations are made for 25 mm radius capsule. Fig. 3(b) shows the solid-liquid interface position predicted by Xia's correlation (Eq. 8) for various m coefficients. R_{int} position predicted by the Raithby's correlation (Eq. 7) is plotted for comparison. As can be seen in the figure, a good approximation is found when the coefficient m is 0.186, which is used to calculate the effective thermal conductivity, and the same approach is extended to predict the appropriate coefficients for other cases.

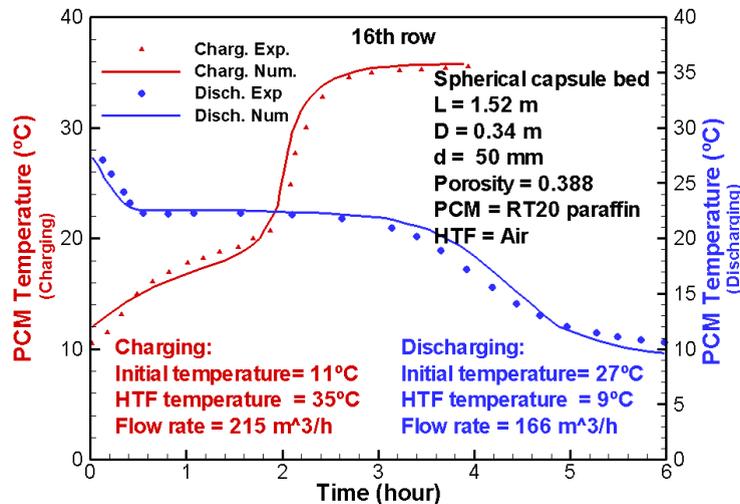


Fig. 4. Experimentally measured [18] and numerically predicted temperature distribution of the PCM capsule at 16th row during charging and discharging processes.

2.3. Validation of the model

For validation purposes, the difference between the numerically predicted results and the experimentally measured results [18] is presented. The experimental results of Arkar et al., [18] are used and the configuration of the system is given in Fig. 4. The temperatures of the PCM capsule at the 16th row of the axis during charging and discharging processes are shown in Fig. 4 for two different flow rates. A good agreement is found between the present numerical results and the experimental measurements.

3. Results and discussion

To study the effect of capsule size on the performance of the thermal storage system, the gas flow rate and the HTF temperature are fixed and simulations are performed for the packed bed filled with various capsule sizes, by assuming the tank wall is insulated. The phase change is assumed between 578.95 and 579.95 K (mushy zone).

Charge mode: 529.95 K is initially considered throughout the tank, which is 50 K (ΔT) lower than the melting temperature, $T_m = 579.95$ K. When $t > 0$, the HTF temperature and the flow rate at the inlet are fixed at 629.95 K and $1 \text{ m}^3/\text{h}$ respectively.

Discharge mode: Initially, the storage tank is assumed as fully charged state, at 628.95 K. When $t > 0$, the temperature of the HTF and the flow rate at the inlet are given as 528.95 K and $1 \text{ m}^3/\text{h}$ respectively. For these conditions, simulations are performed for the packed bed composed of different capsule radii: 10, 15 and 20 mm.

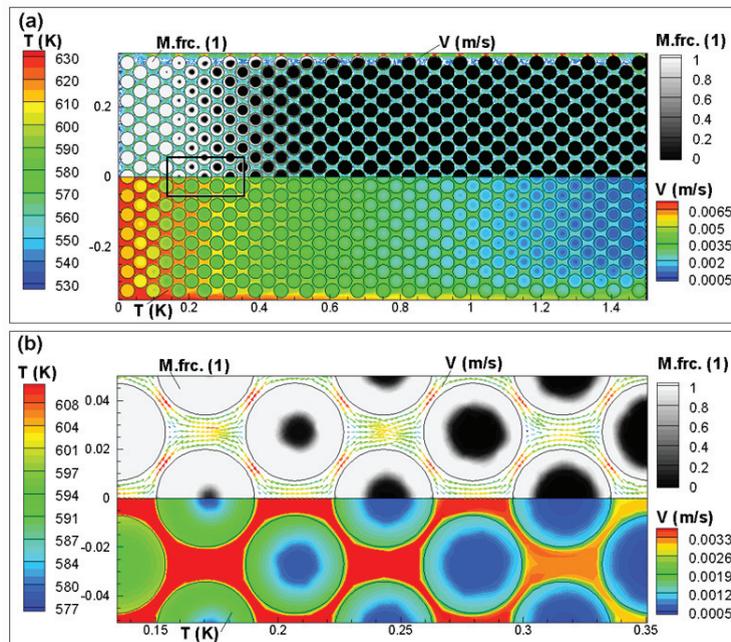


Fig. 5. Temperature, melt fraction and velocity vectors of the storage tank at 1800 s during charge mode

The temperature, melt fraction and velocity distribution of the storage tank at 1800 s during charge mode are shown in Fig. 5, which is composed of 20 mm radius capsules. In Fig. 5 (a), the bottom side represents the temperature distribution of the PCM and fluid domains, and the top side represents the melt fraction of the PCM domain and the velocity vectors of the HTF domain. In order to show the thermal gradients inside the capsule and the corresponding melt fraction, HTF flow around the capsules and the corresponding velocity vectors, a small portion of Fig. 5 (a) is expanded and shown in Fig. 5 (b). It is observed that, this model not only provides the accurate results than continuous solid phase model, but it enables to obtain more details of the fluid flow and heat transfer characteristics of the system. The temperature distribution and melt fraction of the packed bed during charge

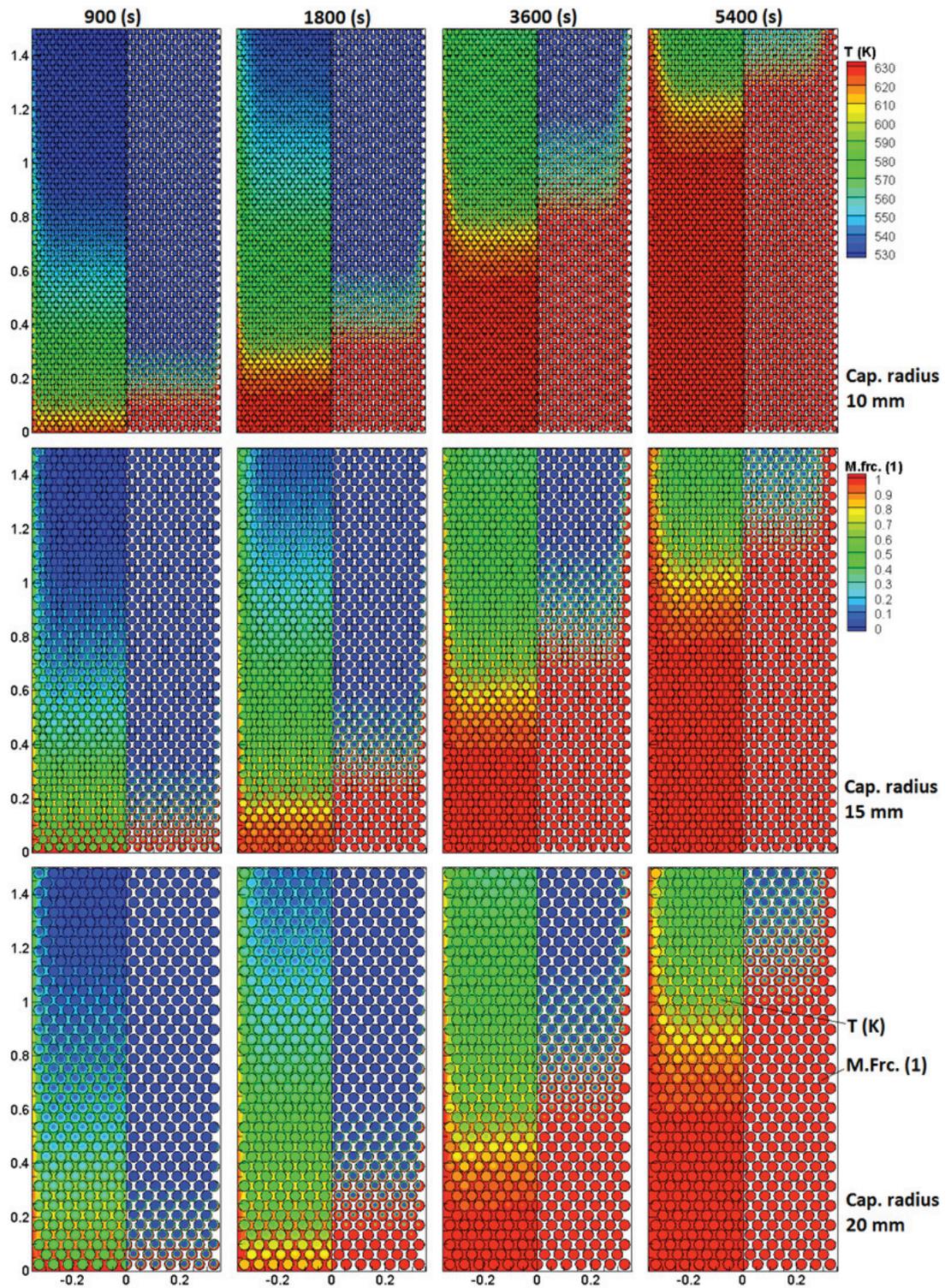


Fig. 6. Temperature and melt fraction of the packed bed during charge process for various capsule sizes at 900, 1800, 3600 and 5400 s.

process are shown in Fig. 6 for various capsule sizes at 900, 1800, 3600 and 5400 s. The 1st, 2nd and 3rd rows represent the packed bed filled with 10, 15 and 20 mm radii capsules respectively. In each plot, the left side represents the temperature and the right side represents the melt fraction. It is observed that the heat transfer between the PCM capsules and the fluid is rapid except the phase change region (mushy zone) due to the latent heat transfer and thermal resistance caused by the molten layer. It is also observed that the heat transfer rate at near wall region is high since the velocity of the HTF is high in near wall region than the rest of the region, as a result, the melting initially started close to the inlet-wall region and gradually spread throughout the tank. This effect is observed in all cases. It can be seen that the heat transfer rate of the bed is high for the small size capsules than the large size capsules.

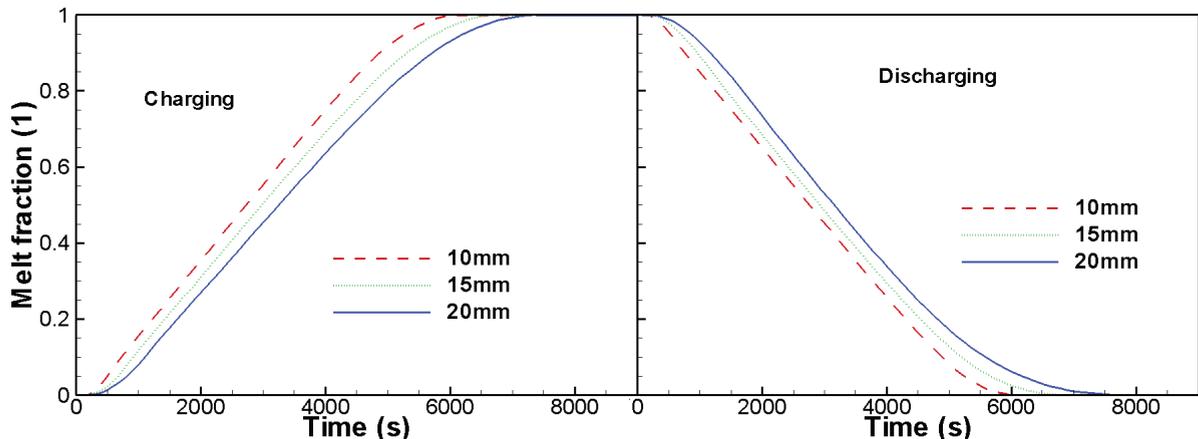


Fig. 7. Melt fraction of the bed during charging and discharging processes as a function of time for different capsule sizes

Melt fraction of the bed during charging and discharging processes is shown in Fig. 7 as a function of time for different capsule sizes. It is noticed that the time for complete melting and solidification is increased when the capsule size is increased. This is due to the heat transfer area between the capsules and the HTF, which is decreased when the capsule size is increased since the surface to volume ratio is decreased. It is also observed that the complete solidification time is longer than the melting time due to the convection effects in the liquid region during melting process.

In order to study the influence of fluid flow rate, capsule radius and ΔT are respectively fixed at 10 mm and 50 K, simulations are performed for various flow rates: 1, 2, 3, 4 m^3/h . The instantaneous temperature distributions of the HTF and the PCM at various axial locations inside the system during charging and discharging processes are shown in Fig. 8.

The heat transfer process at each element of the system generally undergoes any one of the following stages; (1) Constant high temperature stage (CHTS) or the hot stage, when the temperature of the element is at the initial temperature, A-B stage, which is marked in the PCM temperature plot at $1\text{m}^3/\text{h}$ -P2. (2) Constant low temperature stage (CLTS) or the cold stage, when the temperature of the element is equal to the HTF temperature, E-F stage. (3) Heat transfer stage (HTS), which consists of constant melt temperature stage (CMTS), when the temperature of the element is between the mushy zone, C-D stage, and Heat exchange stage (HES), when $T_{\text{init}} < T_s < T_{\text{sol}}$ and $T_{\text{liq}} < T_s < T_f$, two intermediate stages B-C and D-E. These three stages at P1, P2 and P3 are apparently seen in the figure for various cases. In the constant high and low temperature stages, the HTF and the PCM are in thermal equilibrium; in the CMTS, latent energy transfer between the PCM and the HTF takes place; and in the HES, sensible heat transfer between the HTF and the PCM occurs. As estimated, the CMTS and HES are increased when the fluid flow rate is decreased due to the heat transfer rate.

Melt fraction of the bed during charging and discharging processes is shown in Fig. 9 as a function of time for various fluid flow rates. As estimated, the complete melting/solidification time is decreased when the fluid flow rate increased due to the heat transfer rate, which is high for high flow rate.

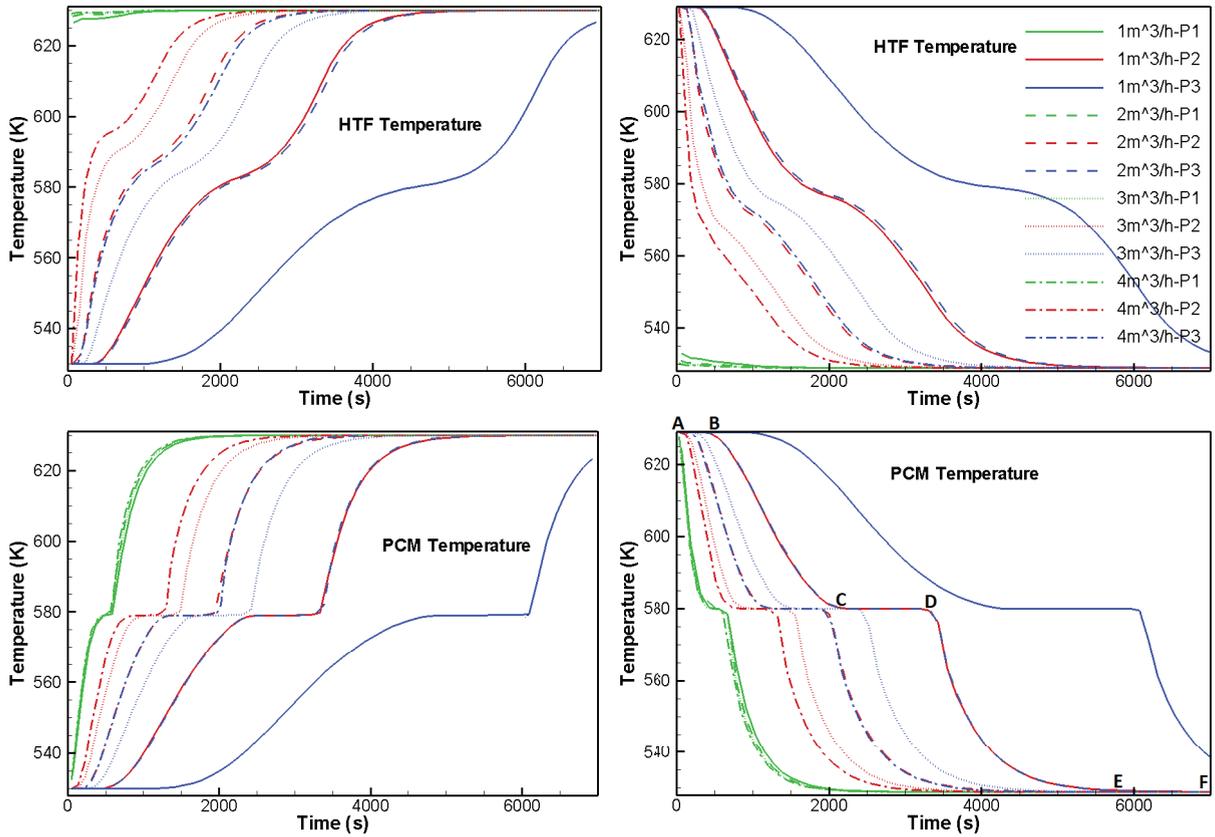


Fig. 8. Instantaneous temperature distribution of the PCM and HTF at P1 (close to the inlet), P2 (centre) and P3 (close to the exit) during charge (left) and discharge (right) processes

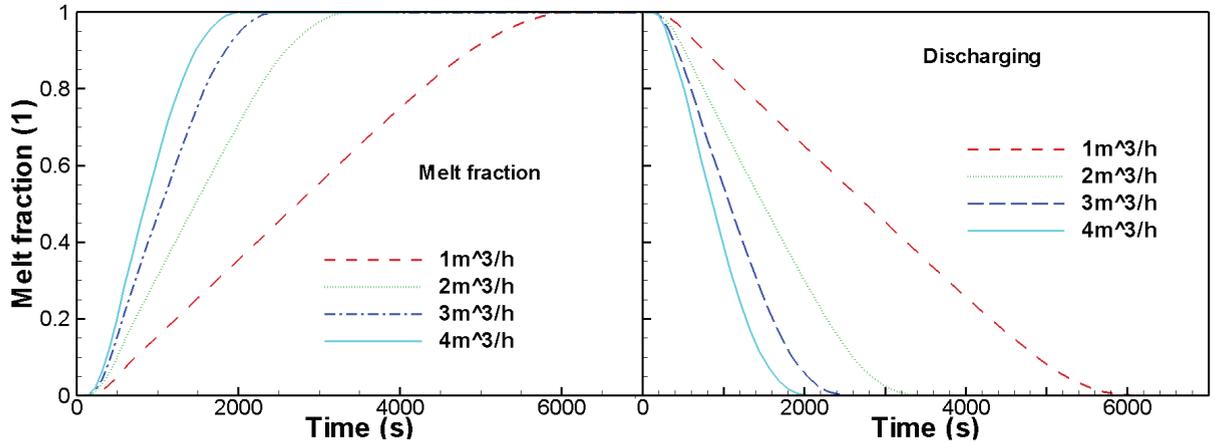


Fig. 9. Temporal variation of melt fraction of the storage tank during charge and discharge processes for various HTF flow rates

4. Summary and Conclusion

The effective packed bed model is developed and used to study the thermal behavior and performance of the TES system. The influence of capsule size and HTF flow rate on the temperature distribution, fluid flow, melting and

solidification of the system is predicted. The following important results are noticed; the heat transfer rate is significantly increased when the capsule size is decreased due to the surface to volume ratio, the complete melting time is shorter than the solidification time due to the convection effects during melting process. This model not only provides the accurate results than continuous phase model, but it enables to obtain more details of the fluid flow and heat transfer characteristics of the system. Thus, this model can be used to optimize the design of the packed bed system and to investigate the influence of operating parameters on the performance of the system.

Acknowledgments

This research was funded by E.ON AG as part of the E.ON International Research Initiative. Responsibility for the content of this publication lies with the authors. In addition, the European commission is acknowledged as well for the research grant through FP7 STAGE-STE Project ‘Scientific and Technological Alliance for Guaranteeing the European Excellence in Concentrating Solar Thermal Energy’ (FP7, Project No. 609 837)

References

- [1] Kuravi S, Traham J, Goswami DY, Rahman MM, Stefanakos EK. Thermal energy storage technologies and systems for concentrating solar power plants. *Progress in Energy and Combustion Science* 2013; 39:285-319.
- [2] Bellan S, Gonzalez-Aguilar J, Romero M, Rahman MM, Goswami DY, Stefanakos EK, Couling D. Numerical analysis of charging and discharging performance of a thermal energy storage system with encapsulated phase change material. *Applied thermal engineering*; DOI: 10.1016/j.applthermaleng.2014.07.009
- [3] Zalba B, Marin JM, Cabeza LF, Mehling H. Review on thermal energy storage with phase change: materials, heat transfer analysis and applications. *Appl Therm Eng* 2003;23:251–83.
- [4] Kenisarin MM. High-temperatures phase change materials for thermal energy storage. *Renew Sustain Energy Rev* 2010; 14: 955–70.
- [5] Garg HP, Mullick SC, Bhargava AK. *Solar thermal energy storage*. Kluwer Academic Publishers; 1985.
- [6] Ismail KAR, Stuginsky R. A parametric study on possible fixed bed models for PCM and sensible heat storage. *Appl Therm Eng* 1999;19:757–88.
- [7] Felix RA, Solanki SC, Saini JS. Heat transfer characteristics of thermal energy storage system using PCM capsule: a review. *Renew Sust Energy Rev* 2008; 12: 2438–58.
- [8] Singh H, Saini RP, Saini JS. A review on packed bed solar energy storage systems. *Renew Sust Energy Rev* 2011;14:1059–69
- [9] Xia L, Zhang P, Wang RZ. Numerical heat transfer analysis of the packed bed latent heat storage system based on an effective packed bed model, *Energy* 2010; 35: 2022–2032.
- [10] Alawadhi EM. Numerical analysis of a cool-thermal storage system with a thermal conductivity enhancer operating under a freezing condition. *Energy* 2008; 33:796-803.
- [11] Tan FL, Hosseinizade SF, Khodadadi JM, Fan LW. Experimental and computational study of constrained melting of phase change materials (PCM) inside a spherical capsule. *International Journal of Heat and Mass Transfer* 2009; 52: 3464-72.
- [12] Bellan S, Gonzalez-Aguilar J, Romero M, Rahman MM, Goswami DY, Stefanakos EK, Couling D. Numerical analysis of packed bed thermal energy storage system for concentrating solar power plants, 2013 ISES Solar World Conf. Proc. (2013) SWC2013-ID475
- [13] Felix RA, Solanki SC, Saini JS. Experimental and numerical analysis of melting of PCM inside a spherical capsule, 9th AIAA/ASME Joint Thermophysics and Heat Transfer Conf. Proc.(2006) AIAA-2006-3618
- [14] Raithby GD, Holland KGT. A general method of obtaining approximate solutions to lamina and turbulent free convection problems, *Advances in Heat Transfer* 1975; 11: 265-316.
- [15] Gnielinski V, Equations for calculating the heat and mass transfer in perfused ball at rest shiite lines for medium and large Peclet number (in German: Gleichungen zur Berechnung des Wärme- und Stoffaustausches in durchströmten ruhenden Kugelschüttungen bei mittleren und großen Pecletzahlen), *Verfahrenstechnik* 1978; 12: 363-366.
- [16] Chiu CP, Chen WR. Transient natural convection heat transfer between concentric and vertically eccentric spheres. *International Journal of Heat and Mass Transfer* 1996;39:1439-52.
- [17] Adine HA, Qarnia HE. Numerical analysis of the thermal behaviour of a shell and tube heat storage unit using phase change materials. *Applied Mathematical Modelling* 2009;33:2132-44.
- [18] Arkar C, Medved S. Influence of accuracy of thermal property data of phase change material on the result of numerical model of packed bed latent heat storage with spheres, *Thermochemica Acta* 2005; 438:192-201.